Large-Eddy-Simulation-Based Wind Tunnel Assessments

Marilyn J. Smith
Daniel Guggenheim School of Aerospace Engineering
Georgia Institute of Technology, Atlanta, GA 30332-0150
USA

marilyn.smith@ae.gatech.edu

ABSTRACT

The advent of large-eddy-simulation (LES) approaches in computational fluid dynamics (CFD) has enabled significant advancements to be made in the context of configurations with separation and unsteady wakes. There have been several computational-experimental collaborations to understand these complex phenomena with mixed success. Some of these collaborations are discussed, highlighting successes and examining shortcomings or gaps. Two configurations are primarily focused upon: a complex rotational rotor hub and a ship airwake. This effort includes the examination of inflow and outflow boundary conditions and wind tunnel blockage assessment.

1.0 INTRODUCTION AND MOTIVATION

Computational fluid dynamics (CFD) and computer hardware have reached a level of maturity where computational analyses can be applied to complex fluid mechanics that have eluded understanding in the past. In particular, the advent of numerical methods with large eddy simulation (LES) turbulence closures solved on massively parallel high performance computing (HPC) have opened the door to new innovation.

However, the 1990's concept of a "virtual wind tunnel" based on numerical methods to replace physical wind tunnels has been discarded. Instead, collaborative investigations that combine both computational and experimental experts have made significant strides in dispatching the single investigator paradigm of research. While each approach has shortcomings, synergistic collaborations that leverage their strengths can overcome their weaknesses and advance research outcomes on complex problems.

This collaborative approach has been particularly successful in the vertical lift community in addressing some of the complex issues that hinder design of faster rotorcraft and operation of vehicles on ships. In several instances, concurrent (or a priori) numerical simulations have been key to the identification of problems in wind tunnel experiments,[1,2,3] including the model setup and design, and the effects of scaling (incorrect Reynolds number), blockage, and dynamic assumptions for "real applications."

These more accurate numerical approaches have highlighted the need for additional information from experimentalists. For example, characterization of the wind tunnel turbulence is now relatively commonplace to provide inputs for LES approaches. Many validation efforts also include the wind tunnel test section and test stand, so that more accurate inflow (pressure ratio, boundary layers, inflow unsteadiness) and outflow (pressure ratio) are required.

In this paper, some of these experimental-computational collaborations are discussed, illuminating their successes and examining shortcomings, usually in the form of unknowns or assumptions that may provide incorrect computational simulations. Three configurations in particular are highlighted: a complex rotational rotor hub, a two-dimensional wing undergoing dynamic stall, and a ship airwake.

1.1 Rotor Hub Drag and Wake Investigation

The rotor hub system (hub, control hardware, blade roots) has been assessed to be one of the primary contributors to rotorcraft parasite drag. This drag, along with the drag from the fuselage, is one of the primary limitations to achieving higher flight speeds on helicopter and advanced vertical flight designs. Until recently, CFD has been limited in its analysis of the rotor hub system due to the complex geometries (see for example, Fig. 1-1), multiple reference frame flows, and separated bluff-body wakes.

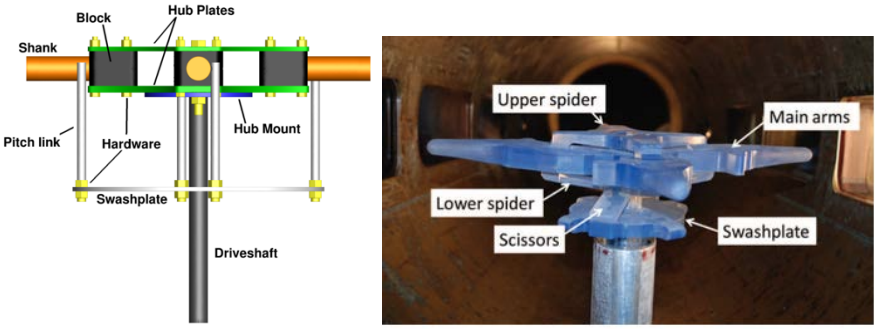

a) Georgia Tech[1] b) Penn State University[4]

Figure 1-1: Example of Rotor Hub Test Models in Recent Experimental-Computational Studies

A collaborative computational-wind tunnel analysis of rotor hub drag and near-body wakes at the Georgia Institute of Technology (GIT) from 2010-2013, resulted several major findings, the most pertinent here that the selection of the experimental model scale was critical due to the many differently-sized components.[1,3] Model-scale simulations of the wind tunnel configuration were able to correlate extremely well with experimental results (See Fig. 1-2) for both integrated loads and near wake behavior. However, the results were significantly different when that same CFD process, adjusted for full-scale length and Reynolds number changes. This led to the realization that the drag and wake behavior appeared to be driven by several of the smaller cylindrical component Reynolds numbers, which were subcritical at model scale, but supercritical at full scale. The need to computationally model the rotation was also observed, as the contribution and wake of different components changes between a static and dynamic assessment, as illustrated in Fig. 1-2. The computations – performed *a priori* to seeing the experimental results – indicate that the flow wake features are correctly captured. A translational shift in some locations is present in Fig. 1-2 (and has been observed in multiple other wake analyses). To ensure that these small shifts do not result in erroneous conclusions about the computations, when "Virtual hot wire" data are collected during simulations for correlation to an experimental hot-wire location, a cloud of data should be saved so that potential translations in the flow features can be assessed.

Reich et al.[5] have published a comprehensive review of the computational and experimental assessment of rotor hub systems. Research at ONERA and US industry confirmed the need to assess the dynamic behavior of the hub system, as both the system performance and the near wake content experienced significant changes. Scaling considerations should include the rotor speed to capture the wake unsteady content. As expected, cylindrical and spherical components are sensitive to Reynolds number scaling, while components with fixed-point separation are not.

These earlier findings led directly to the development of an experimental-computational workshop on a new realistic hub configuration. In this effort, the scaling effects were mitigated through the use of a water tunnel to

provide Reynolds numbers that were above critical values. Furthermore, the necessity of assessing the ability of these CFD solvers to capture longer-age wakes so that rotor-empennage-tail interactions could be evaluated early in the design phase of new vehicles was recognized. The first hub drag workshop was held in June, 2016, and a series of papers on the results of the workshop were presented at the 2017 American Helicopter Society (AHS) Forum.[6,7,8] The sensitivity of the computational predictions to mesh spacing, turbulence model, and solver boundary conditions were documented.

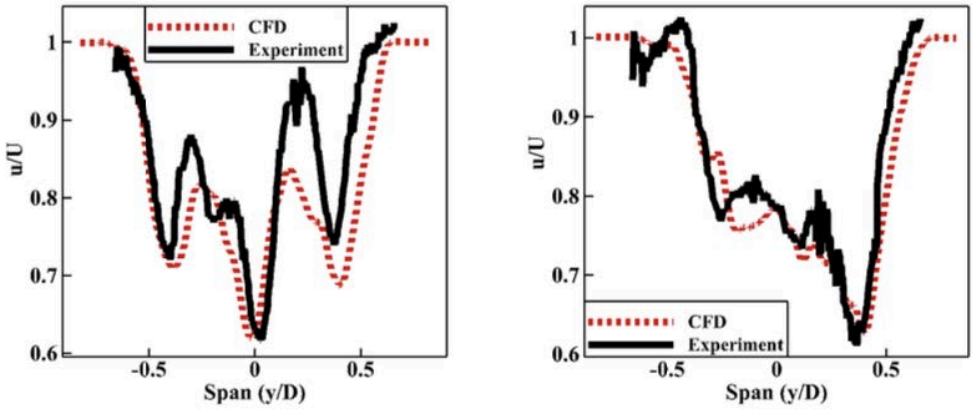

a) Static hub at 0º orientation b) Counter clockwise rotating hub at 240 rpm

Figure 1-2: Comparison of time-averaged PIV and CFD GIT hub centerline wake velocity deficits at one hub diameter downstream along the tunnel axis. From Ref. 1.

An important observation from both the GIT hub drag effort and the PSU hub workshop was that the benefit was not simply the addition of an experimental dataset for computational validation. The computational results, especially when available from multiple solvers, meshes and/or users, were able to guide the experimental effort about potential errors, as well as identify new areas of interest. This interaction has provided a richer understanding of the physics, in particular for the hub workshop effort.

1.2 Ship-Airwake Investigation

Naval air operations occur in the airwake of ships during take-off and landing. This wake consists of massively separated flow embedded with shear flows, vortices, turbulence and transient gusts. Safe operations demand the testing and certification of each ship-aircraft combination at representative wind-directions, which can be an expensive process. Wind tunnel testing at full-scale Reynolds number is prohibitive, but even relaxing that constraint leaves other tunnel effects, notably blockage by the ship model, as well as local wall interference. CFD can provide predictions at full-scale Reynolds number and without blockage or wall-effects, but the simulation must accurately model turbulence, which can lead to the need for extensive computer resources.

For research into naval air (especially helicopter) operations, a “simple frigate shape” (SFS) was proposed and standardized,[9] allowing comparable experiments[10] and computations.[11,12] Later investigations determined that the original geometry missed features shed from the bow of an actual frigate, resulting in the SFS2 geometry (Fig. 1-3). This new model has also been tested in experiment[13] and several computational methodologies including URANS,[14] DES,[15] and hybrid URANS-LES solver methods.[16]

Recently, a campaign to evaluate general ship modelling practices in wind-tunnel testing was completed.[17] The effort investigated three model scales of the SFS2 geometry at three yaw angles (0º, 60º, 90º) in the Naval Surface

Warfare Center Carderock Division (NSWCCD) 8' x 10' subsonic wind tunnel, as illustrated in Fig. 1-4. The model scales ranged from the largest 1/50th scale (1:50) to the smallest 1/100th scale (1:100), as illustrated in Fig. 1-5 for the 60° yaw orientation. The scaled models and yaw angles impose blockage ratios from less than 1% (1:100 scale) to nearly 10% (1:50 scale), so the Maskell blockage correction method was applied to the experimental data.[18] The experiment provides loads on the SFS2 geometry and fast response probe (FRP) data. These blockage corrections to side force and yaw moment cause data from the different models to approach one value, while corrected values of axial force and roll moment show more variation.

A computational effort has been undertaken to evaluate the 1:50 and 1:100 scale model at 2.9 million ship-length Reynolds number at 0°, 60°, and 90° yaw angle in both the tunnel and free-air to evaluate blockage, local wall effects, and the influence of outflow boundary conditions. In addition to correlation with the experimental data, it is hoped that the numerical simulations can provide additional insight into the flow field behaviour. Full-scale simulations at free-air Reynolds number of 290 million (equivalent to about 60 knots) provide a reference for computing scaling and blockage estimates. Time step size was determined so that volume-point sampling matches the experimental FRP response of 2000 Hz for the 1:50 scale model.

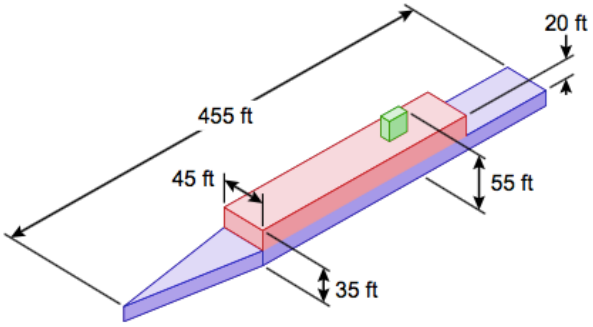

Figure 1-3: Simple Frigate Ship 2 (SFS2) configuration (From Ref. 17)

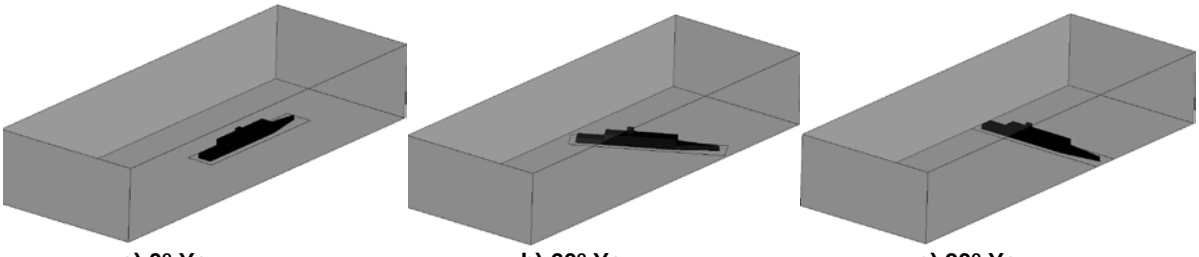

a) 0° Yaw **b) 60° Yaw** **c) 90° Yaw**

Figure 1-4: Orientation of the 1:50 scale SFS2 model in the wind tunnel.

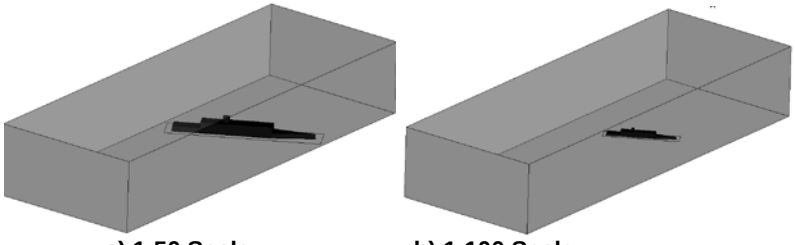

a) 1:50 Scale **b) 1:100 Scale**

Figure 1-5: Comparison of the two SFS2 scale models in the wind tunnel at a yaw orientation of 60°.

2.0 COMPUTATIONAL METHODOLOGY

The CFD solver applied in this study is the FUN3D code developed at the NASA Langley Research Center.[19,20] FUN3D is capable of solving mixed element topological meshes using an unstructured methodology. Second-order backwards differencing provides the temporal discretization, and spatial discretization is also second-order accurate. O'Brien[21] and Renaud et al.[22] have demonstrated that FUN3D's incompressible formulation is not only robust for low-speed flight regimes, but both compressible and incompressible results are comparable to t structured grid results when the grids are locally comparable on the surface and in the boundary layer.

The FUN3D solver was originally developed for fixed-wing applications by NASA researchers. In the early 2000's, overset mesh capability was added in which blade rotations are applied to individual blade grids provide FUN3D's ability to model multiple reference frames of motion simultaneously.[21] In 2015, FUN3D was successfully demonstrated as a new near-body CFD solver within the CREATE-AV HELIOS framework,[23] increasing its footprint for relevant problems in the vertical flight community.

Relevant research efforts have been performed by the author on configurations that include static and dynamic bluff bodies;[2,16] rotating complex hubs, rotors and propellers;[5,6] and dynamic airfoils and wings with separation and reattachment.[24,25] These investigations have resulted in a secondary observation to the original research goals: large eddy simulation (LES) turbulence closures are required to accurately capture the unsteady wake features and the separation. In the present context, the term *LES* is used to refer to either a LES simulation throughout the simulation or a hybrid closure where unsteady Reynolds-Averaged Navier-Stokes (URANS) are rigorously[a] coupled with LES equations to provide LES predictions in a separated wake. These LES approaches require the solution of one or more additional partial differential equations: the turbulent kinetic energy (k) equation and, in some solvers, a turbulence length (l) equation.[26] While LES methods capture transition naturally, hybrid approaches may or may not incorporate transition modelling.[27] Comparisons of traditional unsteady Reynolds-averaged Navier-Stokes (URANS) turbulence models, such as the Menter kw-SST two-equation model, and detached eddy simulation (DES) based on one- or two-equation URANS turbulence models, have been observed to have weaknesses when modelling the separated wakes of static models,[24,28,29] as illustrated in Figs. 2-1 and 2-2. Here, it is demonstrated that the URANS approaches cannot predict the unsteady wake behaviour shed from the cylinder (Fig. 2-1a). Thus, the URANS methods do not capture the point of separation, and thus the integrated drag coefficient is in error by over 50% (Fig. 2-1b). This behaviour is not limited to traditional bluff bodies.

Aerodynamic configurations, such as wings, at high angles of attack encounter similar issues. The RANS methods do not capture the pressure distribution over the leeward portion of the airfoil where separated flow is present, as illustrated in Fig. 2-2 for an airfoil at high angle of attack. As further reported by Hodara et al. for separated flow over a semi-infinite wing at high angle of attack in reverse flow,[24] DES approaches can predict the integrated aerodynamic variables, but tend to temporally smear the wake features. In addition, DES remains more sensitive to the local mesh quality and time step size compared to traditional subgrid-scale LES.

Therefore, the simulations presented in this work are based primarily on the hybrid RANS-LES methodology of Sanchez-Rocha: an additive blending of the Menter SST RANS approach with a one-equation kinetic energy LES formulation, sharing a hybridized turbulent kinetic energy variable.[30] Hodara subsequently added transition, new filters that better protect the boundary layer and capture unsteady features with the local dynamic kinetic energy

[a] Unlike most hybrid RANS-LES approaches, this model includes important cross derivative terms that arise in the derivation of the combined turbulence equations so that the momentum layer between the URANS and LES governing equations are physically correct. This is important for flows such as wind tunnel wall boundary layers.

model (LDKM), and include hybridization terms.[27, 31] The cost of this turbulence closure is approximately 2-3% higher than the original two-equation model for structured solvers and about 5% for unstructured solvers.

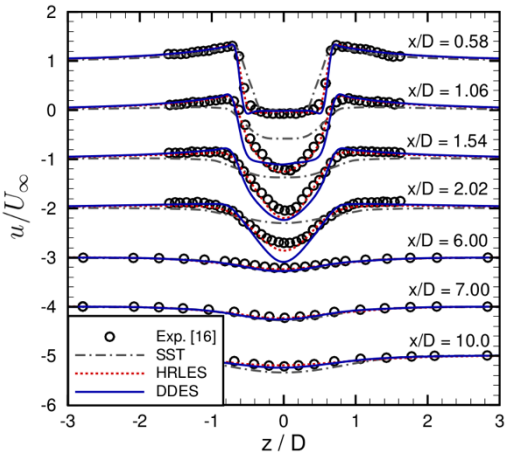

a) Transitional separated wake

Model	Mean C_D	Strouhal no.	Sep. Angle
SST	1.58	0.238	98.4°
HRLES	1.05	0.210	86.7°
LES	1.04	0.210	88.0°
LM	1.35	0.230	96.5°
tHRLES	1.03	0.209	88.0°
Expe.	0.99 ± 0.05	0.215 ± 0.005	$86° \pm 2°$

b) Integrated performance characteristics

Figure 2-1: Correlation of different turbulence simulations on a semi-infinite circular cylinder at Reynolds number of 3,900 (based on cylinder diameter) for a two-equation URANS closure, Delayed Detached Eddy Simulation (DDES) and the hybrid URANS-LES. From Refs. 27 and 31.

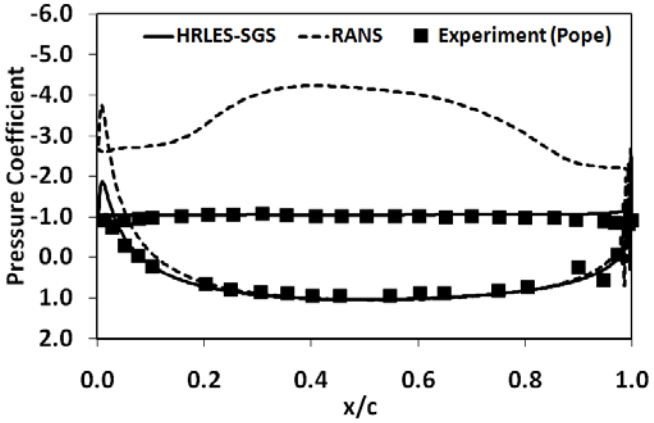

Figure 2-2: Illustration of the importance of a LES turbulence closure in a highly-separated flow about a NACA0012 airfoil at 90º angle of attack. The RANS closure results indicate significant suction on the leeward side of the airfoil, which is not present in the experiment or the HRLES results. From Ref. 32.

2.1 Ship-Airwake Mesh Definition and Simulation Parameters

The meshes of the configuration were determined based on best practices of prior bluff body simulations with unstructured, mixed element meshes.[2,16] Each simulation was comprised of a single mesh that was optimized to the configuration and Reynolds number to avoid errors from oversetting meshes. In typical simulations, a background mesh for the wind tunnel would be developed, and near-body and clustered wake meshes overset. The number of mesh points varied from 20 to 30 million, based on the orientation and location (free air or tunnel). The wind tunnel walls are assumed to be inviscid,[16] so no boundary layer growth was performed. A nominal turbulence intensity of 0.1% was applied to the simulations with a constant velocity inflow and a constant pressure

outflow to mimic the tunnel behavior. Convergence was determined when the change in the drag coefficient of the SFS2 configuration remained less than 1% when evaluated over a 2500 iteration period. This was typically obtained between 14500 and 15000 iterations.

3.0 COMPUTATIONAL ASSESSMENT OF WIND TUNNEL EFFECTS

3.1 Influence of Inflow and Outflow Boundary Condition

Computational simulations of a wind tunnel test section often mimic a standard internal flow with ideal conditions. That is, a constant velocity inflow with a constant pressure ratio outflow over a uniform cross-sectional test section. As CFD simulations are able to more accurately represent actual operations, additional information may be needed to accurately model more realistic wind tunnel inflow and outflow boundary conditions.

3.1.1 Inflow Boundary Conditions

With the use of LES simulations, there are additional considerations that are needed for the computational inflow. The inflow boundary condition is typically a prescribed velocity with computed pressure and density through the perfect gas laws. As LES approaches capture the larger turbulent scales rather than modelling all of the turbulent scales, it is important that the wind tunnel inflow is properly characterized. The turbulence imparted to incoming free stream in the test section needs to be characterized, typically as some form of turbulence intensity. Two recent studies have demonstrated that separation characteristics for both bluff and aerodynamic geometries can significantly be changed with the introduction of turbulence in the flow field.[33,34] These and similar studies provide early assessment of the sensitivity of the simulations to the turbulent and/or small unsteadiness of the inflow, which will likely be increasingly important to measure as the community moves to certification of CFD solvers that will include uncertainty analysis.[35]

3.1.2 Outflow Boundary Conditions

The outflow boundary condition can have a significant impact on the outcome of the computational predictions. The typical computational boundary condition is a pressure recovery ratio, p_{out}/p_{in}, where the pressure at the beginning of the test section, p_{in}, forms the reference of the simulation. As test sections are typically a constant cross-sectional area, it is assumed in many instances that the control volume is sufficiently long to recover the inflow pressure, so $p_{out}/p_{in}=1.0$ if there is no measurement of this pressure.

For the ship-airwake experiments, there were available local velocities in all three axes captured in the test section. As discussed and illustrated by Quon et al.,[16] these were utilized to ensure that the outflow boundary pressure condition was sufficient by correlated with these local test section velocities. The computational simulations indicted that the pressure ratio was approximately $p_{out}/p_{in}=1.0$ for these simulations. In addition, the influence of applying the incompressible versus compressible solution path was explored, as well as using viscous and inviscid wind tunnel walls.

To illustrate the importance of this outflow boundary condition, the pressure ratio was reduced by 10% to $p_{out}/p_{in}=0.9$. There was a noticeable change in the physics observed for these two pressure ratio outflow conditions. Both the minimal blockage case (1:100 scale model at 0^o yaw) and the largest blockage case (1:50 scale model at 90^o yaw) resulted in approximately 2.2-2.5% higher streamwise (drag) force coefficient. The impact of the pressure ratio outflow boundary condition can be observed on the pressure contours over the ship model, as illustrated in Figs. 3-1 and 3-2. While not shown, there are corresponding increases in the magnitude of the fluctuating pressures, in particular on the landing deck of the ship. The pressure distribution along the centerline of the ship also confirms this change.

The influence of the reduced pressure is felt not only on the model, but also in the wind tunnel itself. The pressures along the wind tunnel walls retain their overall shape, indicating blockage as discussed later, but there is a negative translation in the pressure coefficient data indicating the increased speed associated with the pressure gradient at the outflow boundary condition.

While FUN3D had no issues with the outflow boundary condition for this study, and for all the simulations using the wind tunnel configurations, other researchers did find additional sensitivities with the outflow boundary condition. For the hub drag workshop, researchers also applied the OVERFLOW structured solver to the configuration.[7] Here, the outflow boundary condition was based on the mass flow rate, which is a transient and requires a long time to settle and may be subject to significant dissipation within the solver. Approximately 15-16 rotor revolutions were necessary for this outflow parameter to become periodic about a constant value. Conversely, the pressure ratio boundary condition required approximately 9 rotor revolutions to converge.

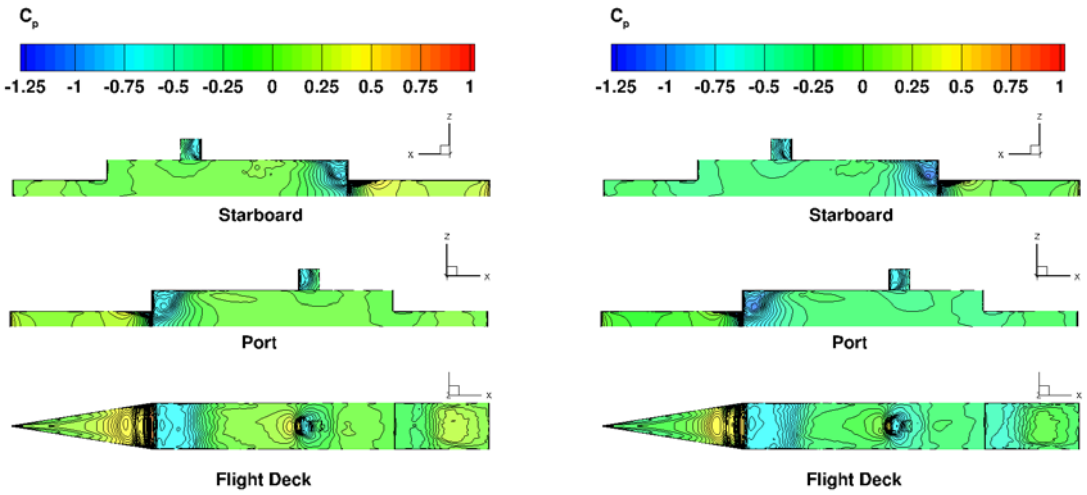

a) p_{out}/p_{in}=1.0 **b) p_{out}/p_{in}=0.9**

Figure 3-1: Influence of the outflow pressure ratio boundary condition on the model pressures for the 1:100 scale model at 0° yaw (minimal blockage).

For both types of outflow boundary conditions, a priori knowledge of the mass flow rate or pressure ratio at the downstream edge of the control volume would significantly improve CFD accuracy and initialization during validation.

3.2 Blockage and Scaling

The experimental effort[17] focused on three different size models 1:100, 1:68, and 1:50. The 1:100 scale model was the recommended model scale for wind tunnel testing as the model length was less than one-half the tunnel width, and its blockage was estimated at less than 1%. Alternately, the 1:50 scale model length covers more than 90% of the tunnel width at the 90° orientation angle, and it has a blockage of about 10% for the wind tunnel. The experimental researchers applied the Maskell correction for bluff bodies to the loads on the ship and observed that the side force was invariant with Reynolds number.

For the computational effort, the blockage effects are directly computed based on the streamwise force (nominally drag) to determine how closely the blockage computed by the Maskell correction.[18] First, the configuration was

evaluated both within the wind tunnel and in free air (no wind tunnel). Two different ship model scales, 1:50 and 1:100, were also evaluated in the wind tunnel to evaluate the differences there.

The pressures along the upper surface of the wind tunnel walls provided a clear indication of the blockage. The centerline pressures along the upper wind tunnel are provided in Fig. 3-3 for the 1:100 and 1:50 scale predictions. For the 1:100 scale model, the pressure coefficient change is minimal, indicating small blockage for all orientations. For the 1:50 scale model, the pressure coefficient change is more significant, in particular for the 90° orientation.

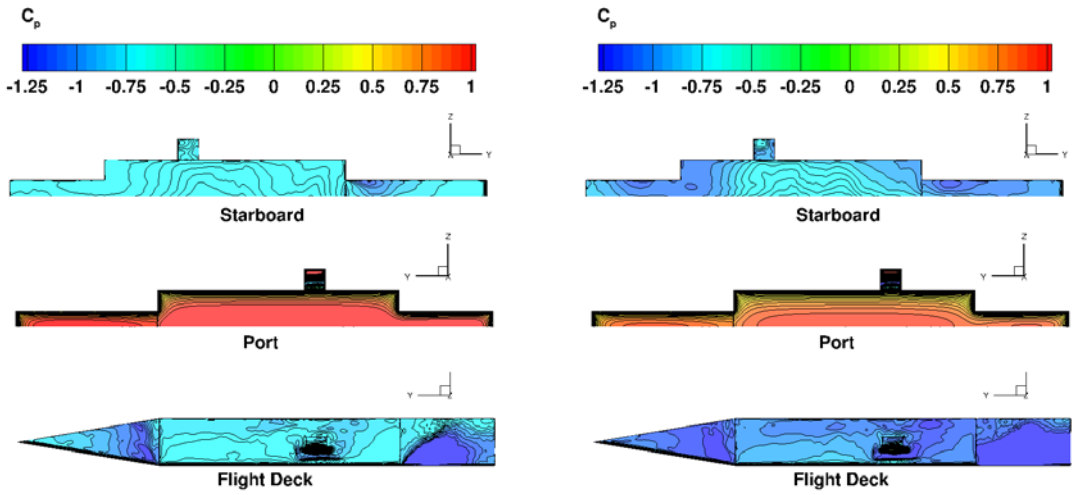

a) p_{out}/p_{in}=1.0 b) p_{out}/p_{in}=0.9

Figure 3-2: Influence of the outflow pressure ratio boundary condition on the model pressures for the 1:50 scale model at 90° yaw (maximum blockage). The port side is windward to the wind tunnel freestream velocity.

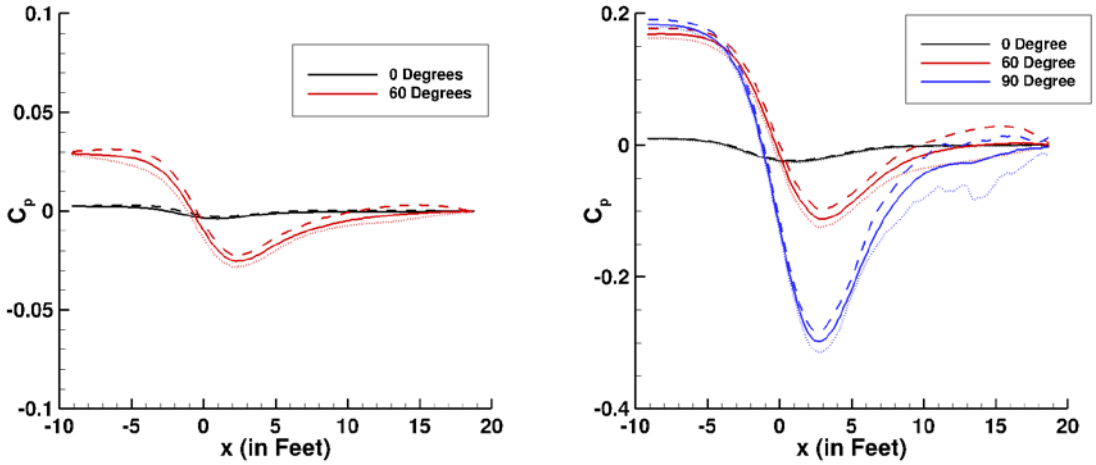

a) 1:100 scale model b) 1:50 scale model

Figure 3-3: Effect of the blockage on the upper wind tunnel centerline, as measured by pressure coefficient.

Another approach to potentially quantify blockage was the comparison of the axial (streamwise) force for free-air simulations with the wind tunnel computations. The comparison with the Maskell blockage estimates from the experiment and simulations are shown in Table 3-1. The Maskell estimates from the simulation, computed using the same assumptions as experiment, tend be larger than the experimental estimates for the smaller scale model (1:100) and smaller for the larger model (1:50). Fluctuations in the computed drag coefficients indicate differences of up to 0.13% for the 0º orientation up to 2.4% for the 90º orientation. These differences are being further assessed.

The results of the direct simulation approach, while there are some differences, are very encouraging when correlated with the experimental Maskell blockage estimates. Most of the estimates are within 1-1.5% of the experimental values, with the largest difference for 1:50 scale model for the 60º orientation. This helps to confirm the conclusion by Rosenfeld et al.[17] that the Maskell approach is appropriate for these ship experiments, but also to assess whether these simulations can be used to help design wind tunnel tests and eliminate costly missteps due to blockage and scaling.

Table 3-1: Comparison of the blockage estimates.

	Maskell (experiment)[17]			Maskell (simulation)			Direct Integration (simulation)		
Model	0º	60º	90º	0º	60º	90º	0º	60º	90º
1:100	+0.45%	+4.68%	+5.59%	+1.36%	+16.1%	--	+0.78%	+3.14%	--
1:50	+2.02%	+21.67%	+28.17%	+1.43%	+18.25%	+23.58%	+3.43%	+16.58%	+28.03%

The computations can further augment the wind tunnel test results by examining more of the details of the flow field. The shed vorticity from the ship superstructures impact the wake through which the landing vehicle must fly. To illustrate, the 0º and 90º cases are examined in Figs. 3-4 and 3-5. There are small differences in the wind tunnel 1:100 and free air model predictions. These are primarily observed on the forward decks. The 1:50 model in the wind tunnel also has minor differences at 0º orientation, but there are significant differences at the 90º orientation. The wind tunnel simulation indicates the presence of significantly larger vortical structures on both the forward and aft decks where the vehicles would be landing. The shear layer from the forward part of the ship is stronger over the aft deck and extends higher. The wind tunnel aft deck also has significantly more vortical structures than the free-air model. The differences in the aft deck behaviour for the 1:50 scale model at the 90º orientation (aft deck is deck on the right of the figure) appears to be influenced by the close proximity of the side wall to the model, with an area of increased velocity over the bow and stern regions, similar to what was reported in the experiment.[17] Similar behaviour was observed for the 60º yaw orientation as well, but is not shown here.

a) Free-air scale model b) Wind tunnel 1:100 scale model c) Wind tunnel 1:50 scale model

Figure 3-4: Visualization of the velocity contours along the plane of the SFS2 centerline to illustrate the effect of the scaling and blockage at 0º orientation. Free stream velocity is from right to left.

a) Free-air scale model b) Wind tunnel 1:50 scale model

Figure 3-5: Visualization of the velocity contours along the plane of the SFS2 centerline to illustrate the effect of the scaling and blockage at 90º orientation. Free stream velocity is into the page.

For these simulations, the tunnel walls have been assumed to be inviscid, as is the usual practice to minimize the cost of modelling the large boundary layer region (see for example, Jain et al.[25]), and as prior evaluations indicated that the viscous boundary layer did not play a role here[16]. However, in other campaigns the wind tunnel wall boundary layer has extended well into the configuration, resulting in the need to model the boundary layer computationally, including an estimate of its thickness at the beginning of the test section, or to remove it as a CFD benchmark (for example, the Research Supercritical Wing database for the Aeroelastic Prediction Workshop[36]).

4.0 DATA MEASUREMENT AND ANALYSIS

While computational simulations with LES wakes at the appropriate temporal and spatial scales have demonstrated their ability to predict the salient features of separated flows, there may exist small time lags and/or spatial translations in the wakes when compared to their experimental counterparts, in particular when configurations undergoing dynamic motion.[24,27] Figure 4-1 illustrates the wake of a static wing in reverse flow where the free stream velocity flows from the trailing edge to the leading edge. The salient features are well captured by CFD with LES wakes, and they appear at comparable times during the vortex shedding cycle, as noted by the nondimensional cycle time noted on the figures. However, when the airfoil is undergoing dynamic motion, such as dynamic stall (Fig. 4-2), there is a time delay during a portion of the cycle when separated flows dominate. Here, the lag is shown in the different times noted between the PIV and computations. These small phase lags can result in differing integrated loads on the body, as the interactions between vortices, shear layers, and other phenomena may be different. Saving instantaneous data during separated flows can help resolve these differences, and lead to further understanding of the complex physics. Monitoring cycle-to-cycle variations of periodic flows can help identify areas where these complex interactions occur so that the computations can be further analysed for these lags.

Time- and phase-averaging of data are primary mechanisms for analysis in wind tunnel tests. For unsteady separated flows, this type of data analysis can potential mask flow features are not fully periodic. An example of this is the nonlinear lift that occurs just prior to stall for a pitching wing. Computations have long predicted that this nonlinear lift is much stronger than experiment, and significant resources have been expended to understand why. In 2014, Ramasamy et al.[37] presented an investigation of experimental data that exhibited this trend. They observed that the onset of the nonlinear lift was not perfectly correlated with the angle of attack. Thus, phase averaging of the data reduced the magnitude of the nonlinear lift peak significantly. Therefore, the computations were predicting the magnitude behaviour correctly.

From the computational analyses and correlations both referenced and newly presented here, the synergy between wind tunnel experiments and computational analyses can be exploited to further understand complex separated flows in the subsonic regime. As discussed in the introduction, these studies have been primarily based upon the author's experience in rotary wing applications, but they are also applicable to fixed-wing applications as well.

As presented earlier for the rotating hub wake, the computations may also present phenomena that are spatially offset by a small amount. Taking experimental hot-wire data at a cluster or row of points may be conducive to helping during CFD validations, in particular if the wind tunnel test section is not to be modelled.

5.0 FUTURE EFFORTS

Additional efforts to understand the rotating hub are underway as part of the second hub drag workshop which will be taking place on May 31, 2018 at Pennsylvania State University in State College, PA USA. Further insights

into the potential use of CFD to design ship-airwake wind tunnel tests are continuing, and the impact of rotating systems on dynamic stall behaviour is also being evaluated.

These efforts have focused primarily on the low Mach number regime, primarily for incompressible or mildly compressible flows. Efforts are planned to further study an accurate, yet efficient approach to model the wall boundary layer, and if a numerically-based blockage correction can be determined for dynamic testing. Gregory[38,39] observed that for his dynamic stall experiments in oscillating free streams that include compressible and transonic effects that a locally varying blockage model is needed.

6.0 ACKNOWLEDGEMENTS

Initial simulations for the ship-airwake and the semi-infinite wing in static and dynamic stall were partially funded through the U.S. Army/Navy/NASA Vertical Lift Rotorcraft Center of Excellence at Georgia Tech under the direction of Mahendra Bhagwat of AFDD, Agreement No. W911W6-11-2-0010. The dynamic stall work was also partially funded under an Army Research Office grant W911NF-13-1-0244; Matthew Munson is the technical monitor. The hub drag research was performed under grant N00014-09-1-1019 from the Office of Naval Research; Judah Milgram was the technical monitor.

Computational time was provided by the Department of Defense (DoD) High Performance Computing Modernization Program (HPCMP). The author would like to thank several graduate students, Philip Cross, Alex Moushegian, Adam Bern, and Siva Movva, in running simulations and post-processing the data for the SFS2 ship-airwake configurations. The efforts of Joachim Hodara and Rajiv Shenoy, graduate students who performed the dynamic stall and hub drag research, respectively, is also recognized. Anya Jones at University of Maryland and Sven Schmitz at Penn State University have been invaluable experimental collaborators in many of the efforts discussed herein. They have been invaluable in their willingness to discuss new ideas and approaches to strengthen experimental-computational synergy.

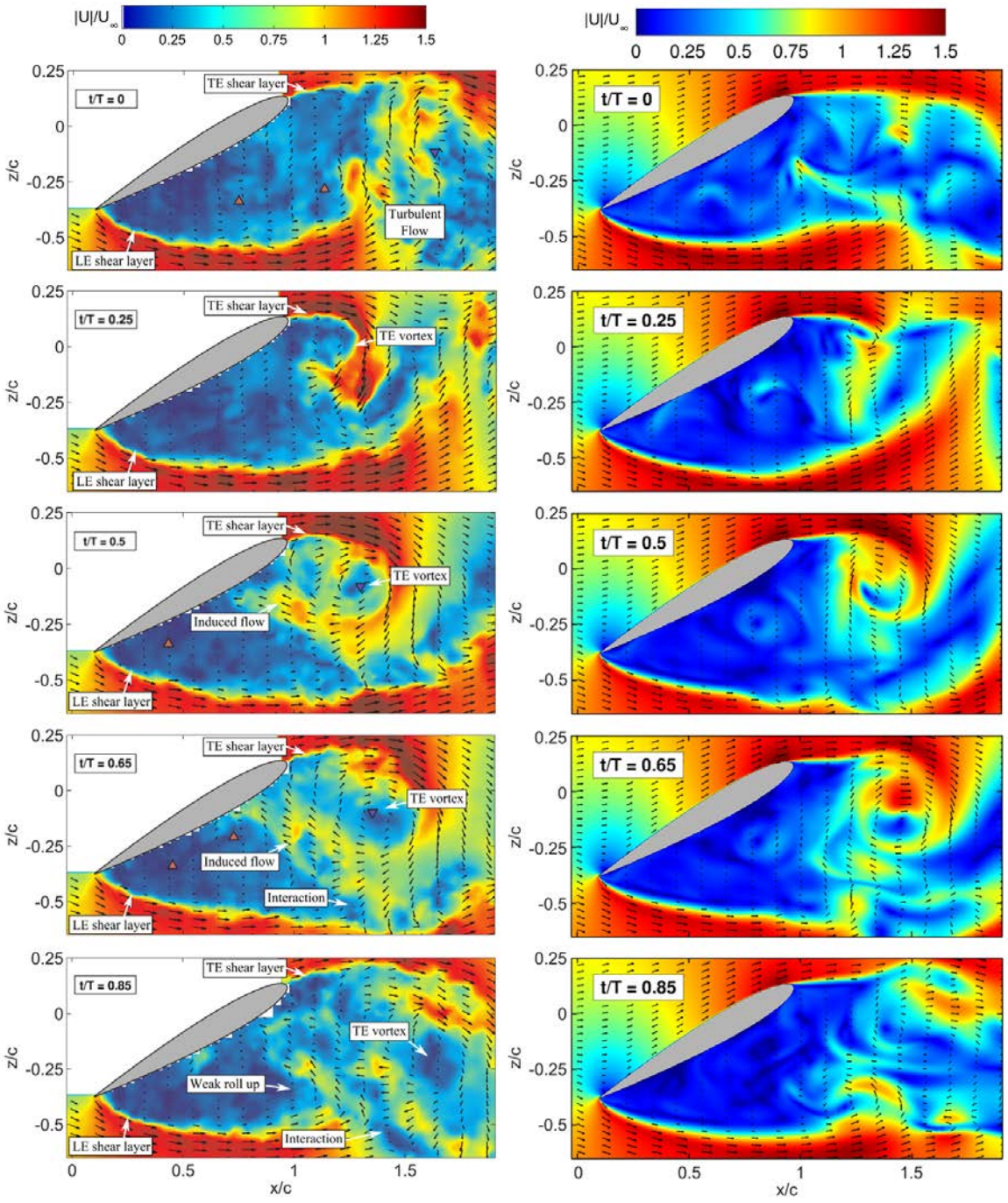

Figure 4-1: Comparisons of instantaneous velocity magnitude contours between PIV measurements (left) and numerical simulations (right) for a static NACA0012 airfoil at Re=1.1x10^5 and α=30^o at various times during the vortex shedding cycle. PIV data from Jones (UMD). From Refs. 24 and 27.

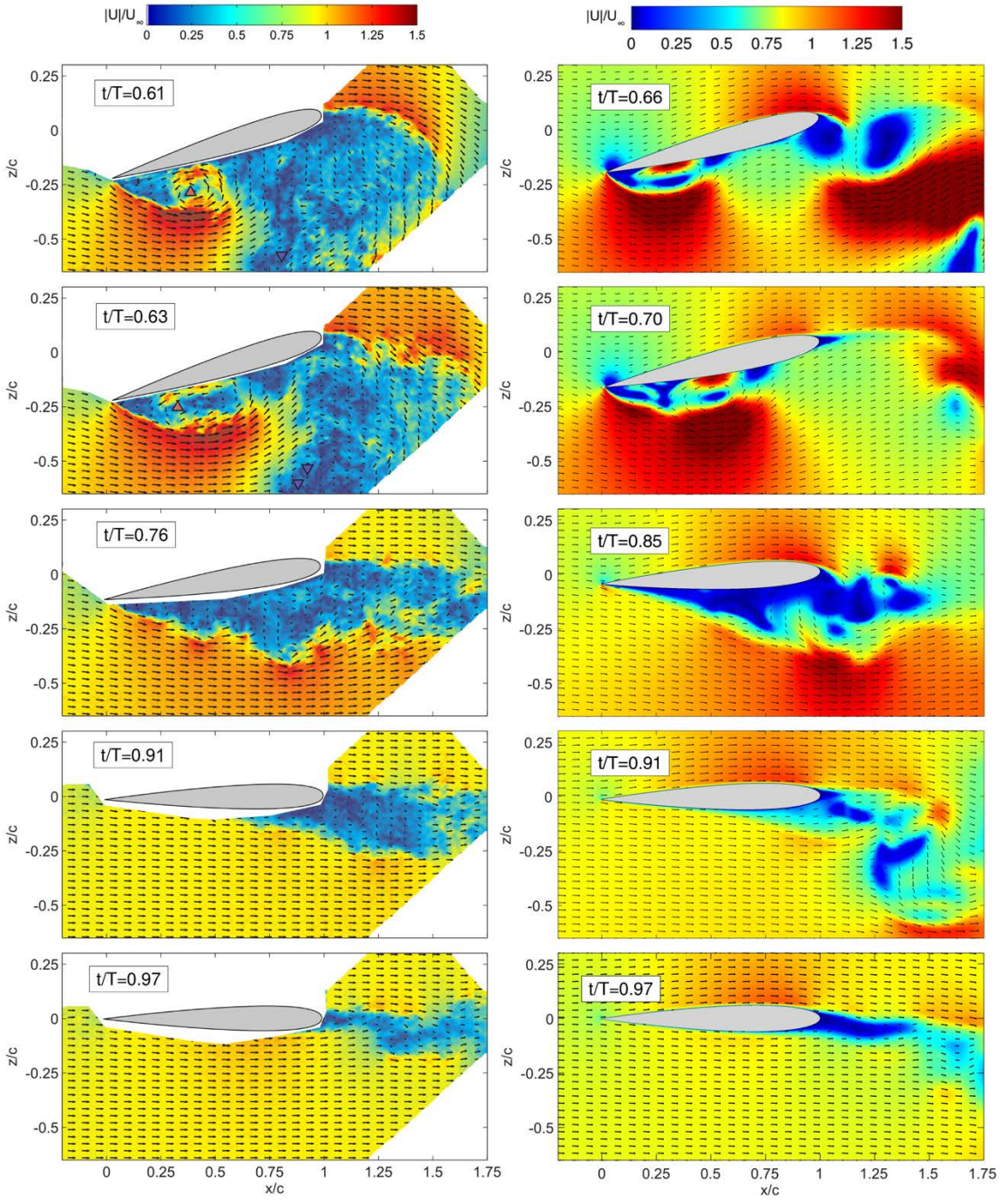

Figure 4-2: Comparisons of instantaneous velocity magnitude contours between PIV measurements (left) and numerical simulations (right) for a NACA0012 airfoil undergoing dynamic pitching oscillations at k=0.16 for at Re=1.65x10^5 and α=10^o +/- 10^o during the second half of the pitching cycle when flow is separated. PIV data from Jones (UMD). From Refs. 24 and 27.

7.0 REFERENCES

[1] Smith, M. J. and Shenoy, R., "Deconstructing Hub Drag: Computational Assessment," Final Report for ONR Project, 2013.

[2] Prosser, D. T., Advanced Computational Techniques for Unsteady Aerodynamic-Dynamic Interactions of Bluff Bodies, Ph.D. thesis, Georgia Institute of Technology, Atlanta, Georgia, https://smartech.gatech.edu/handle/1853/538

[3] Shenoy, R., Holmes, M., Smith, M., and Komerath, N., "Scaling Evaluations on the Drag of a Hub System," Journal of the American Helicopter Society, Vol. 58 (3), 2013, pp. 1-13.

[4] Reich, D. B., Elbing, B. R., Berezin, C. B., and Schmitz, S., "Water Tunnel Flow Diagnostics of Wake Structures Downstream of a Model Helicopter Rotor Hub," Journal of the American Helicopter Society, Vol. 59 (3), July 2014, pp. 1-12.

[5] Reich, D., Shenoy, R., Schmitz, S., and Smith, M. J., "A Review of 60 Years of Rotor Hub Drag and Wake Physics: 1954-2014," Journal of the American Helicopter Society, Vol. 61, No. 1, pp. 1-17, 2016, doi: 10.4050/JAHS.61.022007.

[6] Schmitz, S., Reich, D., Smith, M. J., and Centolanza, L. R., "First Rotor Hub Flow Prediction Workshop Experimental Data Campaigns and Computational Analyses," in Proceedings of the American Helicopter Society 73rd Annual Forum, Ft. Worth, TX, May 9-11, 2017

[7] Coder, J. G., Cross, P. A., and Smith, M. J., "Turbulence Modeling Strategies for Rotor Hub Flows," Proceedings of the 73rd AHS Forum, May 9 – 11, 2017, Fort Worth, TX.

[8] Potsdam, M., Cross, P., and Hill, M., "Assessment of CREATE-AV Helios for Complex Rotating Hub Wakes," Proceedings of the 73rd AHS Forum, May 9 – 11, 2017, Fort Worth, TX.

[9] Wilkinson, C., Zan, S., Gilbert, N., and Funk, J., "Modelling and Simulation of Ship Air Wakes for Helicopter Operations - A Collaborative Venture," RTO AVT Symposium on "Fluid Dynamics Problems of Vehicles Operating near or in the Air-Sea Interface," Amsterdam, The Netherlands, 5-8 October 1998.

[10] Zan, S., "Surface Flow Topology for a Simple Frigate Shape," Canadian Aeronautics and Space Journal, 47:33-43, 2001.

[11]Syms, G., "Simulation of Simplified-Frigate Airwakes using a Lattice-Boltzmann Method," Journal of Wind Engineering and Industrial Aerodynamics, 96(6):1197-1206, 2008.

[12]Wakefield, N., Newman, S., and Wilson, P., "Helicopter Flight Around a Ship's Superstructure," Institution of Mechanical Engineers Part G: Journal of Aerospace Engineering, 216:13-28, 2002.

[13]Cheney, B., and Zan, S., "CFD Code Validation Data and Flow Topology for the Technical Co-operation Program AER-TP2 Simple Frigate Shape," Technical Report NRC-IAR-LTR-A-035, National Research Council of Canada, Institute for Aerospace Research, 1999.

[14] Roper, D., Owen, I., Padfield, G., and Hodge, S. "Integrating CFD and Piloted Simulation to Quantify Ship-Helicopter Operating Limits," The Aeronautical Journal, 110(1109):419-428, 2006.

[15]Forrest, J. S., and Owen, I., "An Investigation of Ship Airwakes Using Detached-Eddy Simulation," Computers & Fluids, 39(4):656-673, 2010.

[16]Quon, E. W., Cross, P. A., Smith, M. J., Rosenfeld, N. C., and Whitehouse, G. R., "Investigation of Ship Airwakes using a Hybrid Computational Methodology," AHS 70th Annual Forum, Montreal, Quebec, 20-22 May 2014.

[17]Rosenfeld, N. C., Kimmel, K. R., Sydney, A. J., Schwartz, A. W., and Ramsey, J. P., "An Investigation of Ship Topside Modeling Practices for Wind Tunnel Experiments," Technical Report NSWCCD-80-TR-2016/006, Naval Surface Warfare Center, West Bethesda, Maryland, 2016.

[18]Maskell, E. C., "A Theory of the Blockage Effects on Bluff Bodies and Stalled Wings in a Closed Wind Tunnel," Technical Report: ARC Reports and Memoranda R&M 3400, Aeronautical Research Council, London,1963.

[19]Bonhaus, D., An Upwind Multigrid Method for Solving Viscous Flows on Unstructured Triangular Meshes, M.S. Thesis, George Washington University, 1993.

[20]Anderson, W., Rausch, R., and Bonhaus, D., "Implicit/Multigrid Algorithms for Incompressible Turbulent Flows on Unstructured Grids," Journal of Computational Physics, Vol. 128, No. 2, 1996, pp. 391–408.

[21]O'Brien, D. M., Analysis of Computational Modeling Techniques for Complete Rotorcraft Configurations, PhD Dissertation, School of Aerospace Engineering, Georgia Institute of Technology, May 2006. https://smartech.gatech.edu/handle/1853/10535

[22]Renaud, T., O'Brien, D., Smith, M., and Potsdam, M., "Evaluation of Isolated Fuselage and Rotor-Fuselage Interaction Using Computational Fluid Dynamics," Journal of the American Helicopter Society, Vol. 53, No. 1, January 2008, pp. 3–17.

[23]Jain, R., Biedron, R.T, Jones, W. T., and Lee-Rausch, E.M., "Modularization and Validation of FUN3D as a CREATE-AV Helios Near-body Solver," AIAA-2016-1298, AIAA Aerospace Sciences Meeting, San Diego, CA, January 4–8, 2016.

[24]Hodara, J., Lind, A., Jones, A., and Smith, M. J., "Collaborative Investigation Of The Aerodynamic Behavior Of Airfoils In Reverse Flow," Journal of the American Helicopter Society, Vol. 61 (3), 2016, pp. 1-15.

[25]Jain, R., Le Pape, A., Grubb, A., Costes, M., Richez, F. and Smith, M.J., "High-Resolution Computational Fluid Dynamics Predictions for the Static And Dynamic Stall of a Finite-Span OA209 Wing," Journal of Fluids and Structures, Vol. 78, 2018, pp.126–145.

[26]Fang, Y. and Menon, S., "A Two-Equation Subgrid Model for Large-Eddy Simulation of High Reynolds Number Flows," AIAA Paper 2006–0116, 2006.

[27]Hodara, J., Hybrid RANS-LES Closure for Separated Flows in the Transitional Regime, PhD Dissertation, Georgia Institute of Technology, 2016.

[28]Liggett, N. and Smith, M. J., "Temporal Convergence Criteria for Time-Accurate Viscous Simulations of Separated Flows," Computers & Fluids, Vol. 66, pp. 140-156, 2012, doi: 10.1016/j.compuid.2012.06.010.

[29]Lynch, C. E. and Smith, M. J., "Extension and Exploration of a Hybrid Turbulence Model on Unstructured Grids," AIAA Journal, Vol. 49, No. 11, pp. 2585-2591, 2011, doi: 10.2514/ 1.56296.

[30]Sanchez-Rocha, M., and Menon, S., "The Compressible Hybrid RANS/LES Formulation Using an Additive Operator," Journal of Computational Physics, 288(6):2037–2062, 2009.

[31]Hodara, J. and Smith, M. J., "Hybrid Reynolds-Averaged Navier-Stokes/Large-Eddy Simulation Closure for Separated Transitional Flows," AIAA Journal, Vol. 55, No. 6, pp. 1948-1958, 2016, doi: 10.2514/1.J055475

[32]Smith, M. J., Liggett, N., and Koukol, B. C. G., "The Aerodynamics of Airfoils at High and Reverse Angles of Attack," Journal of Aircraft, Vol. 48, No. 6, pp. 2012-2023, 2011, doi: 10.2514/1.55358

[33]Maldanado, V., Castillo, L., Thormann, A., and Meneveau, C., "The Role of Free Stream Turbulence With Large Integral Scale on the Aerodynamic Performance of an Experimental Low Reynolds Number S809 Wind Turbine Blade," J. Wind Eng. Ind. Aerodyn.,142(2015), pp. 246–257.

[34]Gaylard, A., Oettle, N., Gargoloff, J., and Duncan, B., "Evaluation of Non-Uniform Upstream Flow Effects on Vehicle Aerodynamics," SAE Int. J. Passeng. Cars - Mech. Syst. 7(2):2014, doi:10.4271/2014-01-0614.

[35]Smith, M. J., Jacobson, K. E., and Afman, J. P., "Towards Certification of Computational Fluid Dynamics as Numerical Experiments for Rotorcraft Applications," Aeronautical Journal, Vol.122, No. 1247, January 2018, pp. 104-130. https://doi.org/10.1017/aer.2017.118

[36]Heeg, J., Chwaloswski, P., Wieseman, C. D., Florance, J. P., and Schuster, D. M., "Lessons Learned in the Selection and Development of Test Cases for the Aeroelastic Prediction Workshop: Rectangular Supercritical Wing," AIAA-2013-0784, 51st AIAA Aerospace Sciences, Grapevine, TX, 7-10 January 2013. https://doi.org/10.2514/6.2013-784

[37][Ramasamy, M., Wilson, J. S., McCroskey, W. J., and Martin, P. B., “Measurements Toward Understanding and Characterizing Cycle-to-Cycle Variations in Dynamic Stall,” presented at the AHS Specialists’ Conference on Aeromechanics Design for Vertical Lift, San Francisco, CA, Jan. 20-22, 2016.

[38]Hird, K., Frankhouser, M., Naigle, S., Gregory, J., and Bons, J., “Study of an SSC-A09 Airfoil in Compressible Dynamic Stall with Freestream Mach Oscillations,” AHS 71st Annual Forum, May 5–7, 2015.

[39]Naigle, S., Frankhouser, M., Gregory, J., and Bons, J., “Effects of Time-Varying Flow Velocity on Steady Blowing Flow Control for a Pitching Airfoil,” AHS 72st Annual Forum, May 17–19, 2016.